Materials Letters: X 1 (2019) 100004

Contents lists available at ScienceDirect

Materials Letters: X

journal homepage: www.elsevier.com/locate/mlblux

Fabrication of β-Mo_2C ultra-thin films by thermal annealing of molybdenum/carbon heterostructures

N. Haberkorn [a,b]

[a] Comisión Nacional de Energía Atómica and Consejo Nacional de Investigaciones Científicas y Técnicas, Centro Atómico Bariloche, Av. Bustillo 9500, 8400 San Carlos de Bariloche, Argentina
[b] Instituto Balseiro, Universidad Nacional de Cuyo and Comisión Nacional de Energía Atómica, Av. Bustillo 9500, 8400 San Carlos de Bariloche, Argentina

ARTICLE INFO

Article history:
Received 10 January 2019
Received in revised form 28 January 2019
Accepted 30 January 2019
Available online 19 February 2019

Keywords:
Carbides
Sputtering
Superconductivity

ABSTRACT

Molybdenum carbide ultrathin thin films are obtained by thermal annealing of molybdenum/amorphous carbon heterostructures. The samples were grown at room temperature by magnetron sputtering on Si (1 0 0). As-grown samples display superconductivity, which could be related to the coexistence of crystalline and amorphous Mo. Interfacial β-Mo_2C phase is observed after thermal annealing at 1033 K. Annealed samples display sharp superconducting transitions. A difference in the maximum critical temperature observed in trilayers and multilayers could be related to superconducting coupling between β-Mo_2C layers.

1. Introduction

Transition metal carbides (TMCs) are formed by incorporating carbon atoms into the interstitial sites of transition metals. They are extremely hard, with very high melting points and high chemical stability [1]. In addition to the excellent mechanical properties, TMCs show excellent surficial catalytic activity [2,3]. Moreover, many TMCs, such as Mo_2C, W_2C, WC, TaC and NbC, exhibit superconductivity [4,5]. The presence of sharp superconducting transitions in thin films with a thickness of a few nanometers makes them good candidates for applications in devices such as single-photon detectors [6].

Superconducting TMCs thin films are usually sintered by chemical and physical methods [7–11]. A distinguishing characteristic of metal carbide / carbon-based composites is the enhancing of the superconductivity at the interface [12,13]. The possibility of stabilizing TMCs at the interface between metals and carbon appears a simple route for the design of superconducting 2D structures.

Among the different candidates for the synthesis of interfacial carbides is the molybdenum. Mo_2C present two different phases: orthorhombic (α) and hexagonal (β) phase. The difference is the distribution of interstitial carbon atoms in the Mo matrix. The superconducting critical temperature (T_c) for bulk is close to 7 K. This value is usually reduced when the film thickness decreases to a few nanometers [7,14].

This letter reports the synthesis β-Mo_2C ultra-thin films by thermal annealing of molybdenum/carbon (Mo/C) heterostructures grown at room temperature. The samples display sharp superconducting transitions for β-Mo_2C layers with thicknesses of a few nanometers.

2. Experimental method

The Mo/C heterostructures were grown by DC magnetron sputtering on (1 0 0) Si. No intentional heating of the substrate was used. The films were obtained from pure Mo and C targets using 50 W and 5 mtorr of Ar gas (purity 99.999%). During deposition, the substrate (typical size 1 cm^2) is positioned directly over the targets at ~5.5 cm. The residual pressure of the chamber was less than 10^{-6} Torr. The growth rate for Mo and C are 33 nm/min and 3.2 nm/min, respectively. The samples were designed with a 2.4 nm thick C buffer layer. Wherever used, the notation $[Mo_t/C_m]_p$ indicates Mo and C layers with thicknesses (nm) of t and m (fixed in 2.4 nm), and p periods. The t value was varied: 1.6 nm, 2.2 nm, 2.8 nm, 3.3 nm, 3.8 nm, and 5.5 nm. Thermal annealing was performed in vacuum (to avoid surface contamination) with a residual pressure of 10^{-5} Torr at 1033 K during 60 min. In order to homogenize the temperature, the films were enveloped in a tantalum foil. The annealing temperature was selected considering crystallization of parent compounds such as molybdenum nitrides [15]. The superconducting properties of as-grown $[Mo_t/C_{2.4}]_1$ are compared with a $[AlN_3/Mo_{2.8}/AlN_3]$ trilayer. The AlN is selected considering its high chemical stability to avoid any chemical

E-mail address: nhaberk@cab.cnea.gov.ar

https://doi.org/10.1016/j.mlblux.2019.100004
2590-1508/

reaction with the substrate and the formation of oxides (MoO_2 and MoO_3) at the contact with the atmosphere [16]. The AlN was grown using the conditions described in ref. [16].

X-ray diffraction (XRD) data were obtained using a Panalytical Empyrean equipment. The thicknesses of Mo and C layers were measured by low angle X-ray reflectivity (XRR). Profile fitting was done using the Parratt32 code [17]. The electrical transport measurements were performed using the standard four-point configuration. The results are separated in trilayers $[Mo_t/C_{2.4}]_1$ and multilayers $[Mo_t/C_{2.4}]_9$. These last ones allow enlarging the intensity of the XRD patterns for phase identification. Multilayers also allow the observation of effects related to superconducting coupling between layers.

3. Results and discussion

Fig. 1a shows the XRD patterns for pure 70 nm thick C and 33 nm thick Mo thin films grown at room temperature. The thicknesses were selected to increase the intensity. The C film is mainly amorphous. It is important to note that no peaks are observed after thermal annealing at 1023 K (not shown). The Mo film displays the (1 1 0) peak corresponding to the BCC structure. As mentioned in the experimental section, the growth rate was calibrated from XRR data in single films. Fig. 1b shows typical patterns and the corresponding fits for a 10 nm thick C film (3.2 nm/min) and a 5.5 nm thick Mo film (33 nm/min). The high amplitude of the oscillations indicates a very low roughness. The thickness fluctuations obtained from the fits are 0.2 nm for Mo and 0.4 nm for C.

The XRD patterns for samples with Mo thinner than 2.8 nm do not display reflections distinguishable from the background, which can be related to size and microstructural effects. The thicknesses of the layers affect the reflections in the XRD (the peak width increases as the thickness reduces). The full width at half maximum (FWHM) predicted by the Scherrer's equation is higher than 4.5° for layers thinner than 2 nm. The observation of reflections in the θ–2θ scans is also affected by the fact that the samples are polycrystalline (reduce the intensity). Fig. 2a shows the XRD pattern for $[Mo_{5.5}/C_{2.4}]_1$. The peak of the as-grown sample could be indexed with the $(1\,1\,0)_{BCC}$ reflection of metallic Mo. The lattice parameter $a = 0.32$ nm is larger than the tabulated value $a = 0.3147$ nm. The annealed sample displays the (1 0 0) and (0 0 2) reflections corresponding to β-Mo_2C. The (0 0 2) peak only appears for $t > 3.8$ nm. The lattice parameters for β-Mo_2C are $a = 0.30$ nm and $c = 0.473$ nm, which agree with JCPDS no. 11–0680. The Scherrer's equation allows the comparison between the grains size along the growth direction and the film thickness. The results using the $(1\,1\,0)_{Mo}$ and $(1\,0\,0)_{Mo2C}$ reflections are 5.8(0.2) nm and 7.5(0.2)

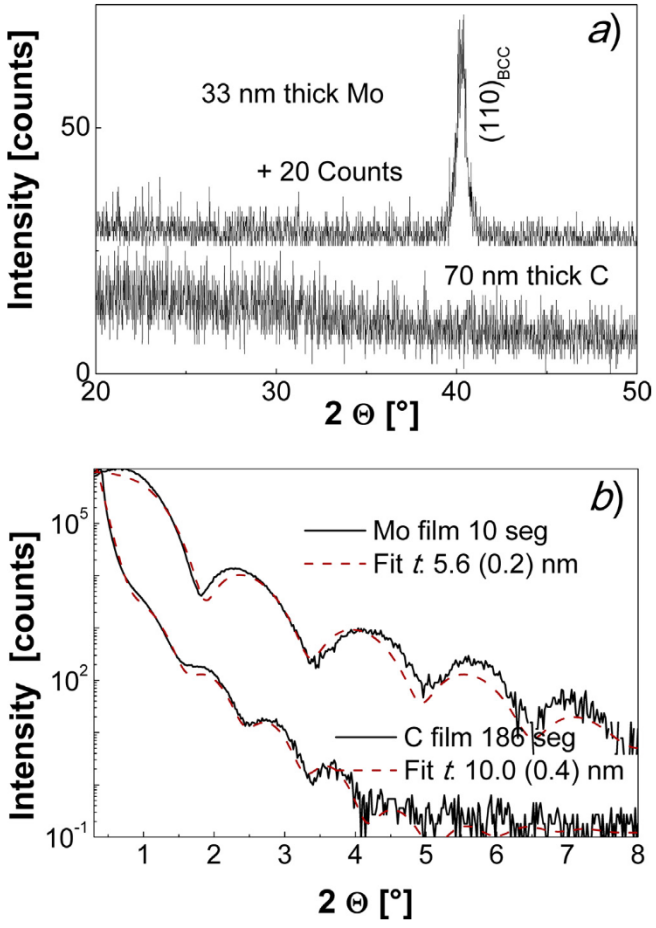

Fig. 1. a-b) XRD and XRR patterns for pure Mo and C thin films, respectively.

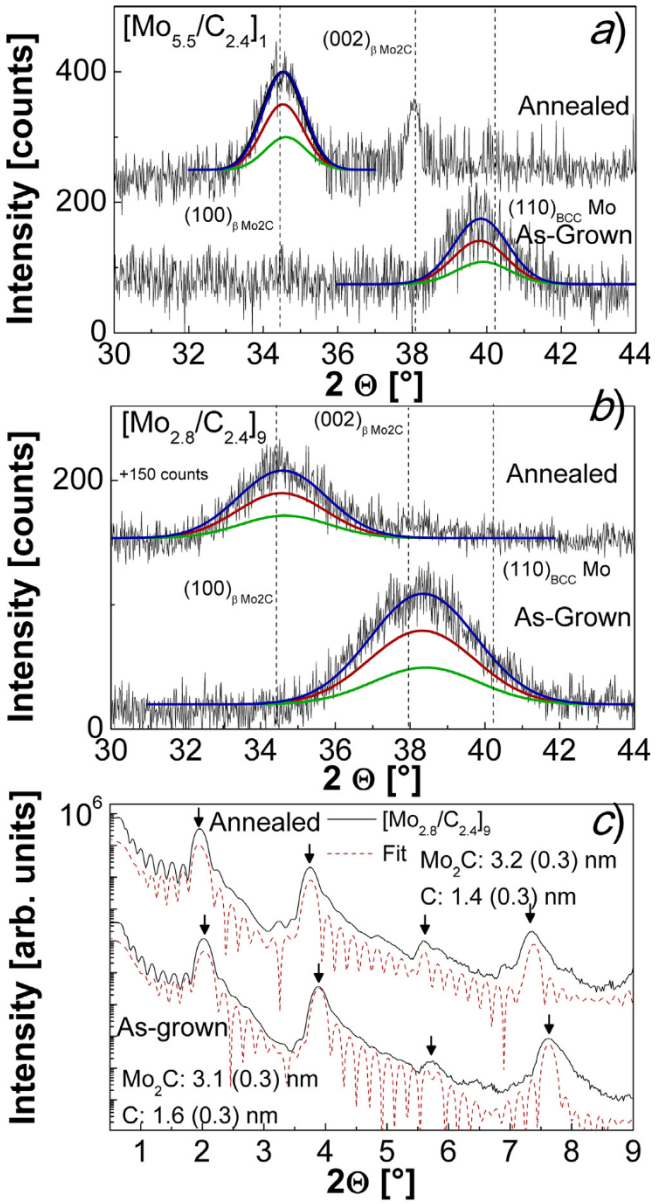

Fig. 2. a) XRD pattern for $[Mo_{5.5}/C_{2.4}]_1$. b) XRD pattern for $[Mo_{2.8}/C_2]_9$. The peaks are deconvoluted using CuKα1 and CuKα2. c) XRR for $[Mo_{2.8}/C_2]_9$. The graph includes the fits with the respective layer thicknesses. For a clearer presentation, the curves were shifted in the y-axis. Arrows indicate the periodicity given by the bilayer.

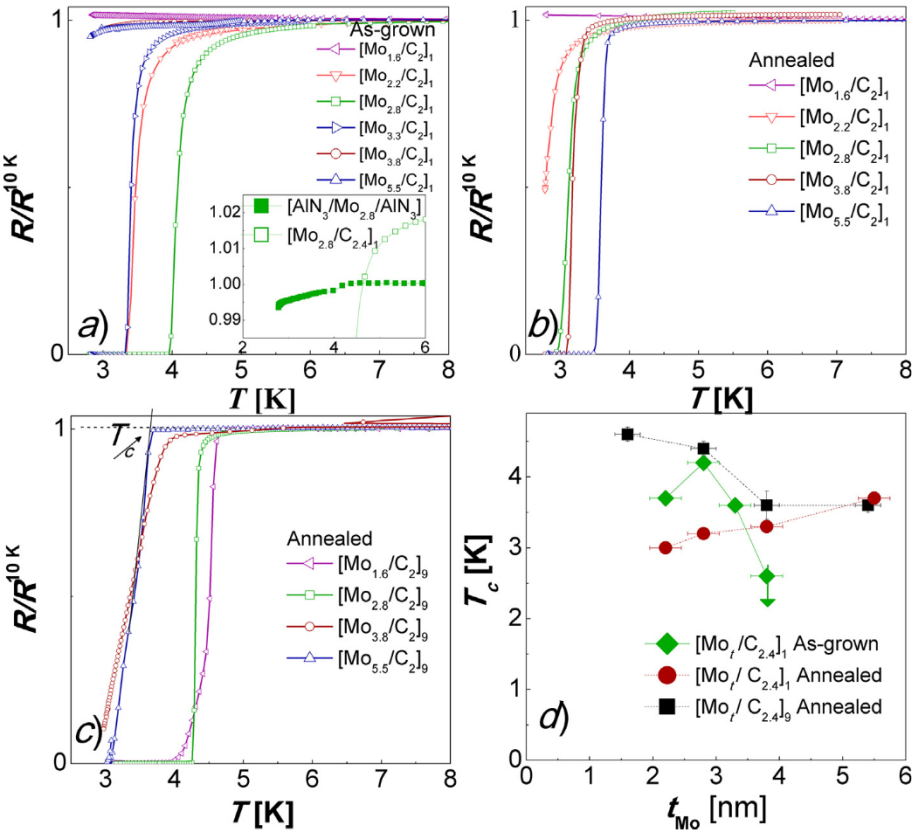

Fig. 3. a–c) Normalized resistance (R/R^{10K}) for as-grown and annealed $[Mo_t/C_{2.4}]_1$, and annealed $[Mo_t/C_{2.4}]_9$, respectively. Inset a) shows the comparison between $[AlN_3Mo_{2.8}/AlN_3]_1$ and $[Mo_{2.8}/C_{2.4}]_1$. d) Summary of T_c values versus nominal Mo thickness (t). The T_c criterion is indicated in c).

nm, respectively. The grain size for the as-grown sample is in agreement with the expected Mo nominal thickness, which indicates that the grains go through the film. The out-plane elongation of the β-Mo_2C grains can be related to the diffusion of C from the interface to the Mo matrix [18]. Fig. 2b shows the XRD for $[Mo_{2.8}/C_{2.4}]_9$. The as-grown sample displays the $(1\,1\,0)_{BCC}$ reflection corresponding to Mo (shifted to lower angles than in $[Mo_{5.5}/C_{2.4}]_1$). The annealed sample exhibits the (1 0 0) reflection corresponding to β-Mo_2C. The grain size (related to the thickness) of the Mo and β-Mo_2C layers are 3.1(0.2) nm and 3.8(0.2) nm, respectively. The enlargement of the β-Mo_2C grains in comparison with pure Mo appears in all the samples that display XRD peaks. Additional structural information can be obtained from XRR data. Fig. 2c shows the XRR for $[Mo_{2.8}/C_{2.4}]_9$. The simulation of the XRR performed with Parrat32 is included. The intensity rapidly decreases followed by an onset with two varieties of periodic oscillations. The maximums indicated by arrows correspond to the Mo/C stacking (distance = thickness Mo + thickness C), showing a periodic structure with modulation in the composition along the growth direction. The oscillations between arrows (at shorter distances) correspond to the total thickness of the sample. The results show that the periodicity of the multilayer can be qualitatively reproduced considering 3.1(0.3) nm thick Mo and 1.6(0.4) nm thick C for the as-grown sample, and 3.3(0.3) nm thick Mo and 1.5(0.3) nm thick C for the annealed one. Although the thicknesses are indistinguishable inside of the error, the best fits correspond to C layers thinner than the nominal value. This fact suggests Mo/C alloying at the interfaces during the growth process. On the other hand, unlike trilayers (with grains going through the film), the presence of maximums related to a periodic structure in annealed multilayers indicates that the chemical reaction between Mo and C take places mainly at the interfaces (no covers homogenously the entire sample).

Following the electrical transport in as-grown and annealed samples is analyzed. The results are summarized in Fig. 3. A distinctive feature is that most as-grown samples display superconductivity (see Fig. 3a). The comparison between $[Mo_{2.8}/C_{2.4}]_1$ and $[AlN_3/Mo_{2.8}/AlN_3]$ indicates that although the superconducting transition could be related to disordered Mo [19], the Mo/C interface is playing a role. The T_c value is higher (with a sharp transition) in $[Mo_{2.8}/C_{2.4}]_1$ than in $[AlN_3/Mo_{2.8}/AlN_3]$ (see inset Fig. 3a). This fact could be associated with both greater disorder and Mo-C bonds stabilizing a superconducting phase. In addition to the disorder, the absence of percolation for $[AlN_3/Mo_{2.8}/AlN_3]$ could be related to slight changes in the roughness. The T_c values change after annealing due to the precipitation of β-Mo_2C. For annealed $[Mo_t/C_{2.4}]_1$, a maximum $T_c \approx 3.7$ K is observed for $t = 5.5$ nm (see Fig. 3b and 3d). The T_c value decreases systematically reducing the Mo thickness, being lower than 3 K for $t = 2.2$. The sample with 1.6 nm does not display features related to superconductivity at the lower measurement temperature (≈2.8 K). This thickness dependence of T_c is similar to that observed in ultra-thin α-Mo_2C single crystals [7]. It is important to note that the superconducting transitions are very sharp (usually T_c-$R^{Zero} < 0.1$ K), indicating high homogeneity and low roughness. The analysis of T_c for annealed $[Mo_t/C_{2.4}]_9$ provides additional information on the microstructure. The transition width in multilayers is usually higher than in trilayers, which could be related to nano-cracks produced by inhomogeneous stress during the recrystallization to β-Mo_2C. Unlike Mo single layers, $t = 1.6$ displays the maximum $T_c \approx 4.6$ K (see Fig. 3c and 3d). The increment in T_c for $t = 1.6$ is the signature of superconducting coupling between β-Mo_2C layers (proximity effects). The T_c value for $t = 5.5$ is similar in $p = 1$ and $p = 9$, which indicates low superconductor interaction between layers. In addition to the coupling, the properties in multilayers could be affected by changes in

the C doping (the C atoms from the spacer diffuse to the bottom and the top Mo layers).

4. Conclusions

In summary, a simple method to fabricate β-Mo_2C thin films is reported. Superconductivity with a sharp transition is observed for films as thin as 2–3 nm. The results suggest that low dimensional superconducting structures based in metal carbides can be easily obtained from metal/C composites, which could include carbon sources such as graphite, nanotubes, and fullerenes.

Conflict of interest

None.

Acknowledgment

This work was supported by ANPCYT (PICT 2015-2171) and CONICET PIP 2015-0100575CO.

References

[1] Elinor Castle et al., Scientific Rep. 8 (2018) 8609.
[2] Xiao Zhang et al., Curr. Opin. Chem. Eng. 20 (2018) 68–77.
[3] Henry Hwu, Jingguang Chen, Chem. Rev. 105 (2005) 185–212.
[4] R.H. Willerns, E. Buehler, B. Matthias, Phys. Rev. 159 (1967) 327–330.
[5] N. Morton et al., J. Less-Common Met. 25 (1971) 97–106.
[6] Chandra M. Natarajan et al., Supercond. Sci. Technol. 25 (2012) 063001.
[7] Xu. Chuan et al., Nat. Mater. 14 (2015) 1135–1141.
[8] Kan Zhang et al., Vaccum 99 (2014) 233–241.
[9] G. Zou et al., J. Am. Chem. Soc. 132 (2010) 2516–2517.
[10] Amit Pawbake et al., Mater Lett. 183 (2016) 315–317.
[11] Hongyang Zhao et al., J. Appl. Phys. 123 (2018) 053301.
[12] G. Zou et al., Nat. Comm. 2 (2011) 428.
[13] Y. Zhang et al., Nanoscale 4 (2012) 2268–2271.
[14] Z. Liu et al., Nano Lett. 16 (2016) 4243–4250.
[15] N. Haberkorn et al., Thin Solid Films 660 (2018) 242–246.
[16] N. Haberkorn et al., Mater. Chem. Phys. 204 (2018) 48–57.
[17] C. Braun, Parratt32 for the Reflectometry Tool, HMI, Berlin, 1997–1999.
[18] W.F. Brizes, L. Cadoff, J. Tobin, J. Nuclear Mat 20 (1966) 57–67.
[19] Shilpam Sharma et al., Physica B 514 (2017) 89–95.